The Astrophysical Journal, 805:69 (14pp), 2015 May 20 doi:10.1088/0004-637X/805/1/69

OBSERVATION OF MUON EXCESS AT GROUND LEVEL IN RELATION TO GAMMA-RAY BURSTS DETECTED FROM SPACE

C. R. A. Augusto[1], C. E. Navia[1], M. N. de Oliveira[1], K. H. Tsui[1], A. A. Nepomuceno[2], V. Kopenkin[3], T. Sinzi[4], and D. Atri[5]
[1] Instituto de Fisica, Universidade Federal Fluminense, 24210-346, Niteroi, Rio de Janeiro, Brazil; navia@if.uff.br
[2] Departamento de Física e Matemática ICT, Universidade Federal Fluminense, 28890-000, Rio das Ostras, RJ, Brazil
[3] Research Institute for Science and Engineering, Waseda University, Shinjuku, Tokyo 169, Japan
[4] Rikkyo University, Toshima-ku, Tokyo 171, Japan
[5] Blue Marble Space Institute of Science, 1200 Westlake Ave N., Suite 1006, Seattle, WA 98109, USA
Received 2014 April 24; accepted 2015 March 23; published 2015 May 20

ABSTRACT

In this paper we examine the possibility of the ground observation of the gigaelectronvolt counterparts associated with the Monitor of All-sky X-ray Image transient event (trigger 58072727) and the *Swift* GRB140512A event. In both cases, there was a muon excess with a statistical significance above 4σ. The coordinates of the events were located in the field of view (FOV) of the Tupi muon telescopes at the time of the occurrence. Since 2013 August, the Tupi experiment has been operating a new extended array of five muon telescopes, located at ground level at ($22\overset{\circ}{.}9S$, $43\overset{\circ}{.}2W$, 3 m above sea level). This location coincides with the South Atlantic Anomaly central region. We consider a hypothesis that the muon excess could be due to photonuclear reactions in the Earth's atmosphere induced by gamma rays with energies above 10 GeV. We describe a data analysis for candidate events identified by internally triggered (by the Tupi experiment) as well as untriggered (dependent on external observations) modes of search. In light of the Fermi LAT (>100 MeV) gamma-ray bursts (GRBs) catalog, we examine the possibility of the ground observation of similar transient events within the FOV of the extended Tupi array and perform a systematic analysis of the Tupi data. Using a Monte Carlo simulation, we discuss the experimental conditions that allow the detection of signals from GRBs at ground level.

Key words: astroparticle physics – gamma-ray burst: general – instrumentation: miscellaneous – telescopes

1. INTRODUCTION

There is some evidence indicating that long-duration gamma-ray bursts (GRBs) occur when very massive stars run out of fuel for nuclear fusion in their cores. The collapse and subsequent intense explosion can rupture a star completely to pieces in a hypernova. Twin beams of gamma rays are hypothesized to burst from the event, and if the Earth is in the path of one of those beams, the gamma-ray burst can be detected. However, in most cases, no narrow gamma-ray lines have been detected. This means that some of these bursts could be produced by the collapse of a massive star without a supernova. Alternatively, the bursts could result from a different progenitor, such as the merger of two white dwarfs or a white dwarf with a neutron star or black hole, possibly in the cluster environment without a host galaxy.

In most cases, spectroscopic analysis on GRBs is consistent with the hard-to-soft evolution as observed by Burst and Transient Source Experiment (BATSE) in bright GRBs (Preece et al. 1998) or by *BeppoSAX* GRBs (Frontera et al. 2000) and the *INTEGRAL* GRB (Gotz et al. 2003).

However, GRB behavior is not universal. This can also be seen in the luminosity distribution of GRBs. For instance, the fluence of the long (20 s) and nearby ($z \sim 0.105$) GRB031203 (Soderberg et al. 2004), observed by *INTEGRAL*, is a factor of 10 smaller than most of the BATSE bright GRBs at cosmological distances. This situation motivates further investigation on whether GRBs can act as standardizable candles.

Many GRB afterglow models (Wang et al. 2001; Zhang & Meszaros 2001; Pe'er & Waxman 2004) predict the production of photons in the gigaelectronvolt to teraelectronvolt energy range, and gigaelectronvolt emission has indeed been detected by previous (EGRET at CGRO; Hurley et al. 1994) and current-generation (Fermi LAT) space-based ray detectors (Abdo et al. 2009).

Among the many remarkable detectors in operation, there is the Monitor of All-sky X-ray Image (MAXI), the first astronomical payload installed on the Japanese Experiment Module-exposed Facility on the International Space Station (ISS; Matsuoka et al. 2009). On 2013 October 15, the MAXI instrument detected an unknown transient source (trigger 580727270) with a preliminary flux of 22.0 ± 0.0 mCrab[6] at the detected position (R. A., decl.) = ($+277\overset{\circ}{.}25$, $-24\overset{\circ}{.}83$). The signal was classified as a GRB or an unknown X-ray transient event. This particular transient event is interesting to the Tupi experiment because it is the second MAXI transient event candidate with coordinates located within the field of view (FOV) of the Tupi telescopes at the time of the trigger occurrence. The previous one was observed in the inclined (45° relative to the vertical) Tupi telescope pointed to the west (Augusto et al. 2013).

On the other hand, *Swift* is a multiwavelength GRB detector (Gehrels 2004), and the Burst Alert Telescope (BAT) covers the 15–150 keV energy band and can detect more than 100 GRBs per year. In addition, *Swift* has the X-ray telescope (XRT) and the ultraviolet and optical telescope (UVOT) to identify and observe X-ray, UV, and optical afterglows. On 2014 May 12, the *Swift* instruments detected a multipeak and bright GRB; the trigger coordinates were very close to the zenith in the Tupi location, and a muon excess in coincidence

[6] http://gcn.gsfc.nasa.gov/maxi_grbs.html. In spite of the negative values in the flux fields, the MAXI messages are considered to be acceptable by the MAXI team.

with the *Swift* trigger time was registered in the Tupi vertical telescope.

The muon excess observed at the ground could be an indication of the high-energy tail of a GRB that might extend up to the gigaelectronvolt energy range. Several scenarios have been suggested to explain a possible high-energy component of GRBs. For instance, the synchrotron self-Compton model (Panaitescu & Meszaros 2000; Kumar & McMahon 2008) provides a natural explanation for the optical and gamma-ray correlation seen in some GRBs. It has also been shown that a relatively strong second-order inverse Compton (IC) component of the GRB spectrum should peak in the tens of gigaelectronvolts energy region (Racusin et al. 2008). Observations by the Tupi experiment can be complementary to other techniques by setting the limits on the strength of this IC peak because some systematic characteristics between the MAXI event and its possible high-energy counterpart at Tupi, as reported in this article, are not far from that expected in light of the systematics of the Fermi LAT (>100 MeV) GRBs (Ackermann et al. 2013).

This article is organized as follows. Section 2 explains the experimental setup, showing that the coordinates of the MAXI trigger 580727270 and *Swift* GRB140512A were within the effective FOV of the vertical Tupi telescope. Section 3 presents an untriggered search for bursts at ground level using the Tupi telescope and describes the methods and the analysis used. We report new results from the Tupi experiment in association with the MAXI and *Swift* instruments. The muon excess fine structure was used for an estimation of the significance and duration of the observed signal. We show that the two events were not spikes of a short duration, but most likely signals with a structure. Section 4 describes how a triggered analysis at ground level can give an alert of a GRB based only on the muon excess input, independent of the extrenally triggered satellite observations. In Section 5, we include a spectral analysis based on a hybrid method that combines a Monte Carlo simulation and analytical calculations. This approach allows us to evaluate the gamma-ray spectrum and fluence associated with the observed muon excess. In Section 6, we examine the possibility of the ground observation of similar transient events within the FOV of the extended Tupi array of five telescopes and perform a systematic comparison between the GRB characteristics, in light of the Fermi LAT (>100 MeV) GRB catalog. Section 7 presents the results of an additional Monte Carlo simulation of the lateral distribution in the atmosphere of photomuons (muons produced in the atmosphere by photoproduction) in different geomagnetic conditions. As an example, we show that in the South Atlantic Anomaly (SAA) region (the Tupi experiment site) the atmospheric lateral spread of photomuons at ground level is narrower and the number of muons is higher in comparison with the Yangbajing International Cosmic Ray Observatory (Tibet, China, 30°.11*N*, 90°.53*E*, 4300 m above sea level). Thus, the low geomagnetic field in the SAA can increase the sensitivity of a muon telescope. Section 8 summarizes our conclusions.

2. TUPI SETUP

Since 2013 August, the Tupi experiment has been operating an extended array of five muon telescopes (Augusto et al. 2011). The first one has a vertical orientation. The other four have orientations to the north, south, east, and west, and each telescope is inclined 45° relative to the vertical. Figure 1 shows the FOV of five telescopes during the occurrence of the MAXI trigger 580727270 on 2013 October 15.

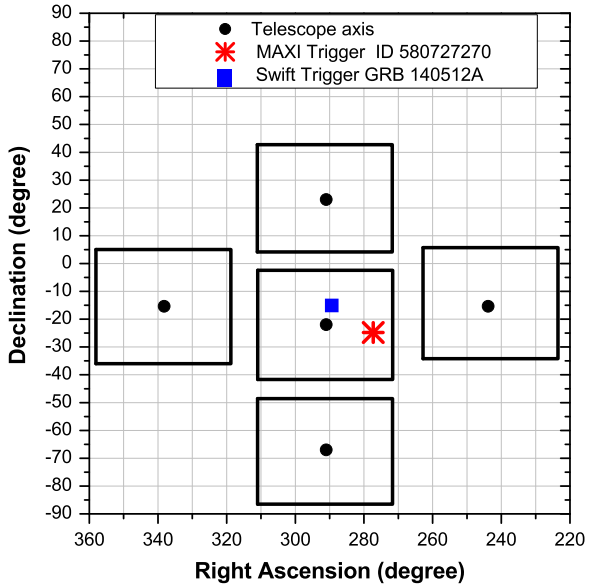

Figure 1. Equatorial coordinates of the Tupi telescope's axes (black circles). Squares represent the effective field of view of the telescopes, and the asterisk is the position (coordinates) of the MAXI transient event (trigger 580727270).

Each telescope was constructed on the basis of two detectors (plastic scintillators 50 cm x 50 cm x 3 cm) separated by a distance of 3 m; one of them is shown in Figure 2.

Each telescope counts the number of coincident signals in the upper and lower detector. The output raw data consists of a coincidences counting rate of 1 Hz versus universal time (UT). The Tupi telescopes are placed inside a building under two flagstones of concrete (150 g cm^{-2}). The flagstones increase the detection muon energy threshold up to the ~0.1–0.2 GeV required to penetrate the two flagstones. Each Tupi telescope - has an effective FOV of $\sim 0.37 sr$. To the vertical telescope, this corresponds to an aperture (zenith angle) of 20° from the vertical.

Time synchronization is essential for correlating event data in the Tupi experiment, and this is achieved by using the GPS receiver. All steps from signal discrimination to the coincidence and anticoincidence are made via software using the virtual instrument technique. The application programs were written using the LAB-VIEW tools. The Tupi experiment has a fully independent power supply, with an autonomy of up to 6 hr to safeguard against local power failures. As a result, the data acquisition is basically carried out with a duty cycle of 95%. The Tupi experiment is in the process of constant expansion and upgrade. Work is underway to set up new telescope sites in Campinas (Brazil) and La Paz (Bolivia).

3. UNTRIGGERED SEARCH FOR A BURST AT GROUND LEVEL

The goal of the transient event search in the Tupi experiment is to identify a significant muon excess of short duration in relation to other observations (Augusto et al. 2012a, 2012b). Usually, this type of search is highly dependent on satellite observations and is the most used by ground-level detectors. In this mode of search, the Tupi data are analyzed for an enhancement in the counting rate with a significance above a

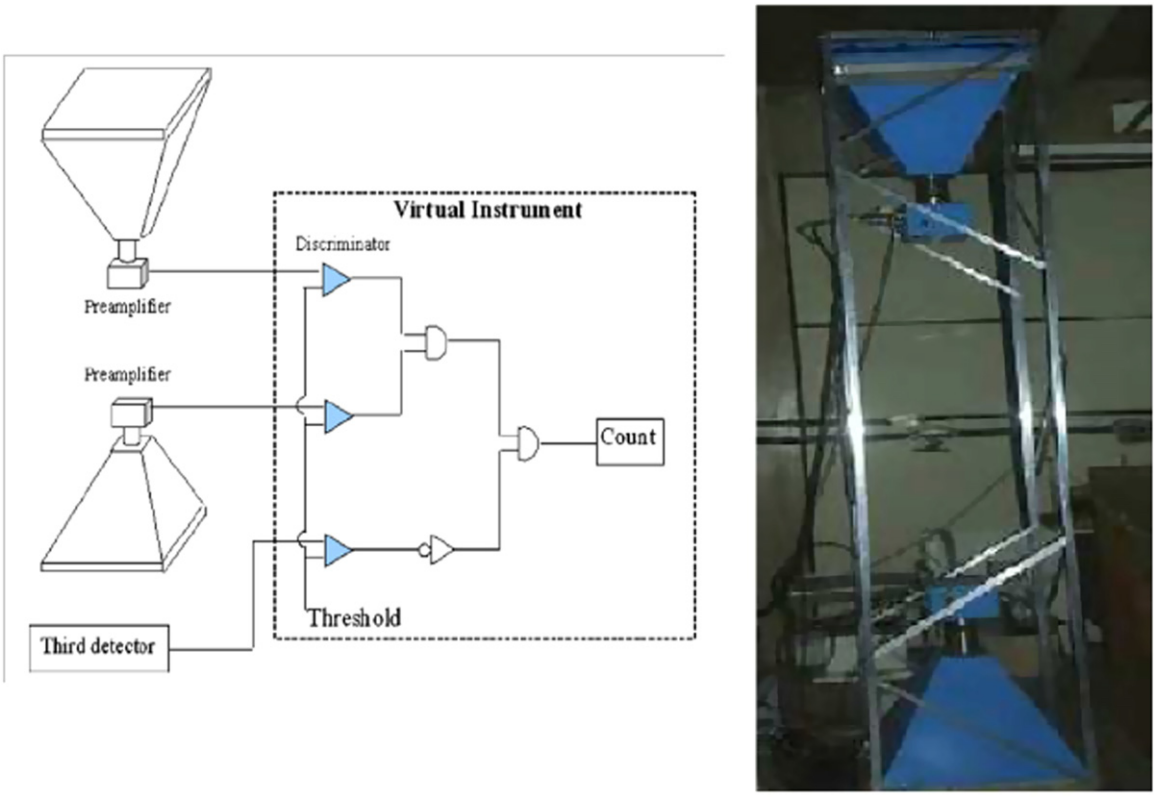

Figure 2. Left: general layout of the vertical Tupi telescope, including the logic in the data acquisition system using the virtual instrument technique. Right: photograph of the vertical Tupi telescope.

given value (4σ) in temporal and spatial coincidence with a transient event detected by satellites. In general, spatial coincidence means that the GRB's coordinates are within the FOV of the ground-level detector. The temporal coincidence means that the signal at ground level must be at least within the T90 duration of the GRB. The duration parameter T90 is the time over which a burst emits from 5% of its total measured counts to 95%. However, the high-energy emission can be delayed with respect to the trigger time, as observed, for instance, by EGRET and Fermi LAT. In some cases, such as the ARGO experiment, the search was extended to several hours around the GRB trigger time (Girolamo et al. 2008). In the Tupi experiment we apply a time window of ± 500 s.

3.1. Tupi Observation Associated with the MAXI Event

On 2013 October 15 at 21:55:44 UT, a peak (muon excess) with a significance of $\sim 5\sigma$ at the 68% confidence level was found in the 24 hr raw data (counting rate 1 Hz) of the vertical Tupi telescope. The Tupi signal significance was calculated according to the bin selection criteria algorithm of Mitrofanov et al. (1999) and Augusto et al. (2010). According to this algorithm, the signal statistical significance S in the ith bin is defined as $\sigma_i = (C_i - B)/\sqrt{B}$ where C_i is the measured number of counts in the ith bin and B is the average background count. It was possible to recognize this peak in the time profile of the muon counting rate just by the naked eye, as shown in Figure 3. The peak was found at $T_0 + 25.7$ s, where $T_0 = 21{:}55{:}19$ UT is the occurrence of the MAXI trigger. In addition, a second narrow peak with a significance of $\sim 4\sigma$ can be observed at $T_0 + 297.2$ s.

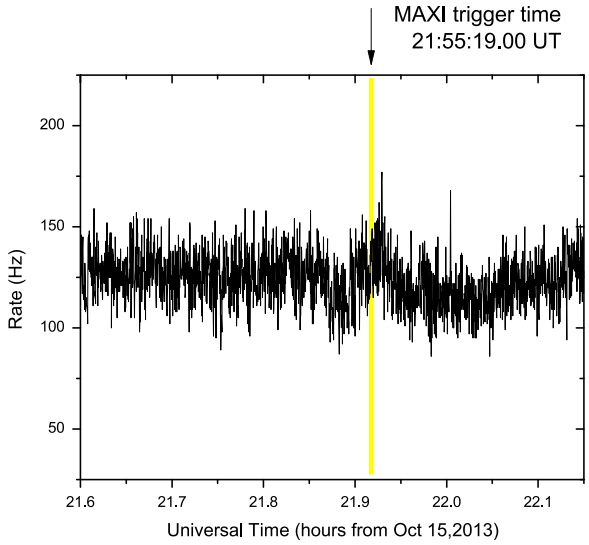

Figure 3. Raw data observed in the vertical Tupi telescope on 2013 October 15 (counting rate 1 Hz). The vertical bold line indicates the occurrence of the MAXI trigger 580727270.

Figure 4 shows in detail the experimental data in the vertical Tupi telescope as a function of time elapsed since the trigger 580727270 signal. The top panel represents the muon counting rate (in Hz) and the bottom panel represents the signal significance measured (in units of standard deviation).

In order to see with more accuracy the background fluctuations, we have examined the time profiles up to half

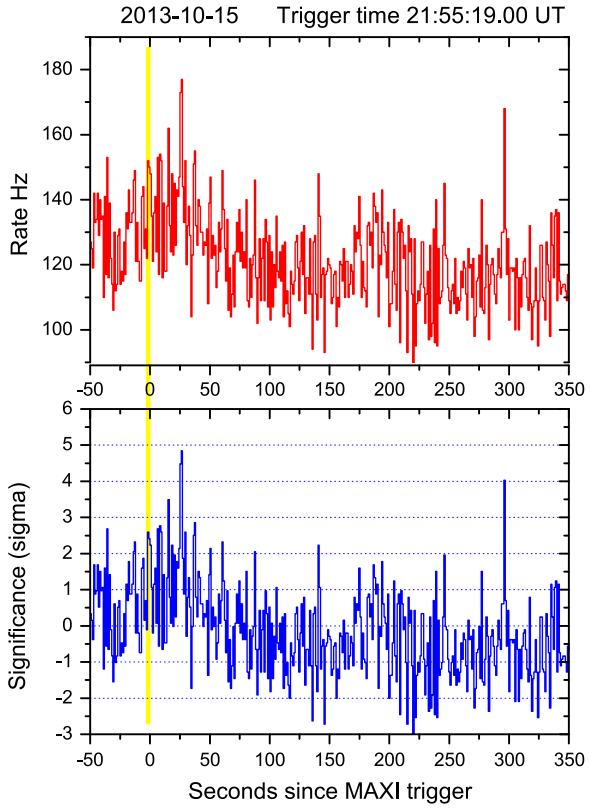

Figure 4. Top panel: the counting rate observed in the vertical Tupi telescope on 2013 October 15. Bottom panel: statistical significance (number of standard deviations) of the 1 s binning counting rate observed by the vertical Tupi telescope, both as a function of the time elapsed since the MAXI transient 580727270 trigger time.

an hour before and after the trigger time because in this time interval the coordinates of the MAXI event are still inside the FOV of the vertical Tupi telescope. For longer time intervals, due to the rotation of the Earth, the coordinates of the trigger are no longer in the FOV of the Tupi telescopes. A confidence analysis has been made for a 1 hr interval around the MAXI trigger time, as shown in Figure 5.

From this analysis, it is possible to identify the Tupi signals with a significance above 4σ associated with the MAXI transient event, and we can see that the tail of the significance distribution is outside the muon background from the galactic cosmic-ray component that follows a Gaussian distribution (solid line).

We would like to point out that in the present case the peak is not a spike of short duration, but a signal with a structure that can be fit by a Gaussian distribution, with an FWHM = 3.9 s. The signal duration is $T_{90} = 6.1 \pm 0.7$ s at the confidence level of 68%, as shown in Figure 6.

In addition, one can notice that there is a second muon excess spike-like peak at $T_0 + 295.3\ s$. This spike with a significance of $\sim 4\sigma$ (1 s binning) can be related to the MAXI event because it can be seen with the naked eye even in the 3 s and 5 s binning counting rates, as shown in Figure 7. This behavior can be a consequence of the broad pedestal.

Table 1 shows several quantities related to these two peaks.

3.2. Tupi Observation Associated with the Swift Event

According to Pagani et al. (GCN 16249), on 2014 May 12 at 19:31:49 UT the *Swift* BAT triggered and located GRB140512A (trigger = 598819), which was also detected by the Fermi Gamma-ray Burst Monitor (GBM; Stanbro GCN 16262). The BAT on board calculated location was (R. A., decl.) = (289.371, −15.100). The BAT (GBM) light curve showed a multipeak event with a total duration of about 170 s. The peak count rate was ∼8000 counts s^{-1} in the energy range 15–350 keV at ∼122 s after the trigger time. Several afterglows were observed to be linked to GRB140512A, such as the *Swift* XRT (Evans et al. GCN 16255), the *Swift* UVOT (Porterfield et al. GCN 16263), as well as several optical afterglows.

A muon excess associated with the *Swift* BAT trigger time, with a significance of $\sim 4.55\sigma$ in the raw data, was observed in the vertical Tupi telescope. There is a peak in the Tupi data from T-12.0 s to T+3.0 s, where T is the *Swift* trigger time. The coordinates of this GRB were very close to the zenith in the Tupi location, within the FOV of the vertical telescope. Figure 8 shows a comparison between the time profiles of the *Swift* GRB140512A and the statistical significance (number of standard deviations) of the counting rate (4 s binning) observed by the vertical Tupi telescope, as a function of the time elapsed since the *Swift* BAT GRB140512A trigger time.

As in the previous Tupi association with the MAXI event, the peak associated with the *Swift* GRB140512A event is not a spike of short duration. The time profiles of the muon counting rate can be seen in Figure 9. In this case the signal persists, with the same confidence, in the 1, 3, 5, and 10 s binning counting rates.

To see the expected background fluctuations, a confidence analysis has been made for a 1 hr interval around the *Swift* BAT trigger time, as shown in Figure 10.

4. TRIGGERED SEARCH FOR A SIGNAL AT GROUND LEVEL

If there is an increase in the muon counting rate and the satellite information on the event location is absent, how can we be sure that this is due to a transient event? An algorithm to search the sky for GRBs has been developed by the Milagro team.[7] In this method, if an excess above the background is observed, the Poisson probability of this excess being due to a fluctuation of the background is calculated.

The Milagro observatory was an extended air shower array, with a wide FOV and high duty cycle, monitoring the northern sky almost continuously in the energy range from 100 GeV to 100 TeV. It was located near Los Alamos, NM, USA, and operated from 2000 January to 2008 May. The Gamma-ray Coordinates Network (GCN) system has incorporated the distribution of positions of GRBs and transients detected by the Milagro instrument. Milagro has succeeded in detecting gamma rays in the teraelectronvolt energy region, such as teraelectronvolt gamma rays from the galactic plane (Abdo et al. 2007b) and the discovery of teraelectronvolt gamma-ray emission from the Cygnus region of the Galaxy (Abdo et al. 2007c). Perhaps its high-energy threshold (above 100 GeV) set for gamma rays did not allow the detection of GRBs, so only upper limits have been reported (Abdo et al. 2007a). We have adapted Milagro's algorithm to the Tupi experimental conditions, as described below.

[7] http://umdgrb.umd.edu/cosmic/milagro_grb_info.html

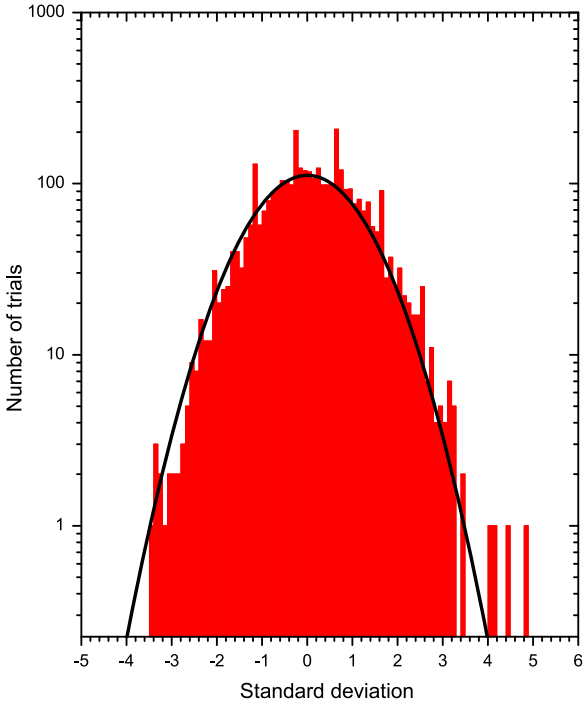

Figure 5. Distribution of the fluctuation counting rate for the vertical Tupi telescope (in units of standard deviations) using 1 s time windows inside a 1 hr interval (30 minutes before and 30 minutes after the trigger) around the MAXI transient event (trigger 580727270). The signals with a significance above 4σ are the Tupi signals associated with the MAXI transient event, and they are outside the background fluctuations represented by the Gaussian distribution (solid line).

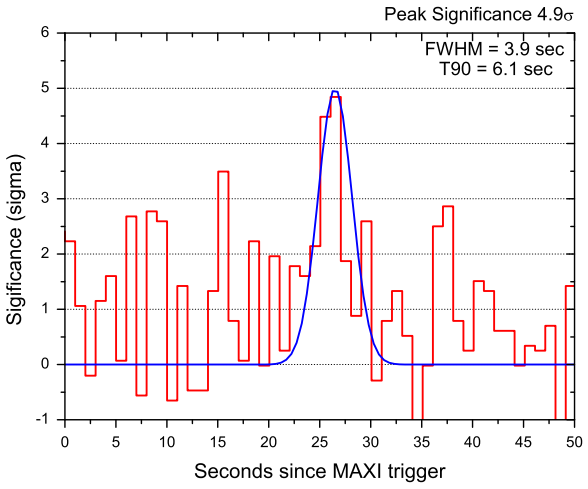

Figure 6. Fine structure of the muon counting rate peak in possible association with the MAXI trigger 580727270. This signal is consistent with a Gaussian distribution with an FWHM of 3.9 s.

4.1. Counts in a Fixed Interval

It is useful to express the Poisson distribution in a form that can be readily applied to the analysis. If the average number of events in a time interval Δt is μ, then it is convenient to define a counting rate by the quantity $r = \mu/\Delta t$. The probability of observing exactly ν events in Δt is then given by the Poisson

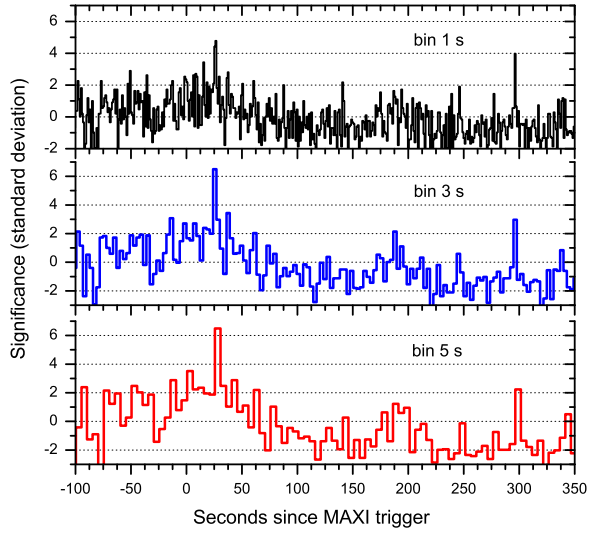

Figure 7. Statistical significance (number of standard deviations) of the 1, 3, and 5 s binning counting rates observed by the vertical Tupi telescope, as a function of the time elapsed since the MAXI transient 580727270 trigger time.

distribution function with mean $\mu = r\Delta t$:

$$P_{r\Delta t}(\nu) = \frac{(r\Delta t)^{\nu}}{\nu!} e^{-r\Delta t}. \quad (1)$$

Assuming there are no astrophysical signals in the Tupi data (a typical quiet day), we can search through 24 hr of data and count the number of times we see a fluctuation over the background. For each ($r\delta t$) bin, the Poisson probability that the observed excess was due to a background fluctuation is calculated, and the probability distribution is determined. Figure 11 shows this distribution for two different temporal bin widths; the top panel is for a 1 s bin and the bottom panel is for a 5 s bin.

In the untriggered search for GRBs (see Section 3), in association with a satellite GRB trigger, a muon excess with a significance above 4σ in the raw data set (bin = 1 s) is considered to be a candidate event. The Poisson probability of an event with a significance of 4σ being a background fluctuation is $P = 1.9 \times 10^{-4}$ or $\log_{10}P = -3.7$, and following Figure 11 (top panel) one can see that there are eight events per day (2920 per year) satisfying the criterion. However, these events look like spikes, with a duration no longer than 2 s. Such spikes, at least in part, can be produced by the (high-energy component) particle precipitation coming from the inner Van Allen belt because the Tupi location is within the SAA (see Section 7).

On the other hand, at least two events (analyzed here) show that the signal persists in temporal bins of different duration (see Figures 6 and 8). For instance, if the 5 s bin is used, then the Poisson probability of the 4σ event being a background fluctuation is $P = 7.4 \times 10^{-6}$ or $\log_{10}P = -5.1$. From Figure 11 (bottom panel), using the linear fit, one can find that there are 0.2 events per day (73 per year) satisfying the criterion. In principle, this type of Tupi data analysis can be used to generate GRB and transient event alerts, independent of the satellite GRB triggers.

We estimated the Poisson probability of a muon excess observed in the vertical Tupi telescope, in association with the MAXI and *Swift* GRB events, being a background fluctuation,

Table 1
Characteristics of Peaks Observed by the Tupi Experiment in Possible Association with the MAXI Trigger (580727270)

MAXI–Tupi association				
Peak Time (s)	Significance	T90 (s)	Muon Excess	Fluence (erg cm^{-2})
T_0 + 25.7	~5.0σ	6.1	39.1 ± 7.2	(2.1 ± 0.4) × 10^{-7}
T_0 + 297.2	4.0σ	1.0	16.5 ± 3.3	(7.1) × 10^{-10}

Note. The trigger time is T_0. The duration parameter T90 is the time over which a burst emits from 5% of its total measured counts to 95%.

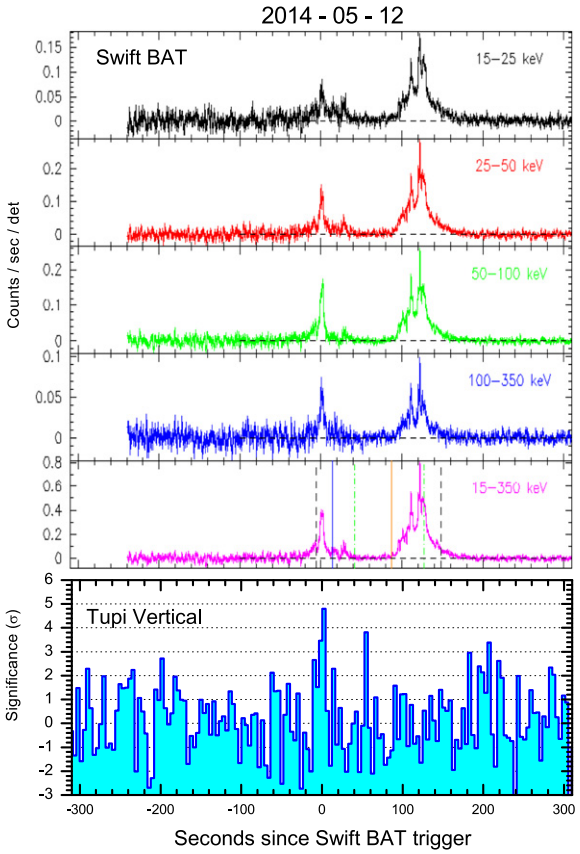

Figure 8. Top five panels: the counting rate of gamma rays in five energy ranges for the event GRB140512A observed by the *Swift* BAT. Bottom panel: statistical significance (number of standard deviations) of the 4 s binning counting rate registered by the vertical Tupi telescope, as a function of the time elapsed since the *Swift* BAT GRB140512A trigger time.

as well as the expected annual rate. The results are presented in Table 2.

5. SPECTRAL ANALYSIS

The observed energy spectra of gamma-ray bursts reveal a diverse phenomenology. The spacecraft observed gamma rays up to 33 GeV (Abdo et al. 2009). While some energy spectra can be fitted by a simple expression over many decades (Abdo et al. 2009b), others require a few separate components to explain the high-energy emission (Abdo et al. 2009). In most cases (at low energies), the GRB spectrum is well described by a phenomenological "band function" in a "Comptonized model" using a power law with an exponential cutoff:

$$N(E) = kE^{\alpha}e^{-E/E_0}, \quad (2)$$

where α is the power-law exponent and E_0 is the cutoff energy .

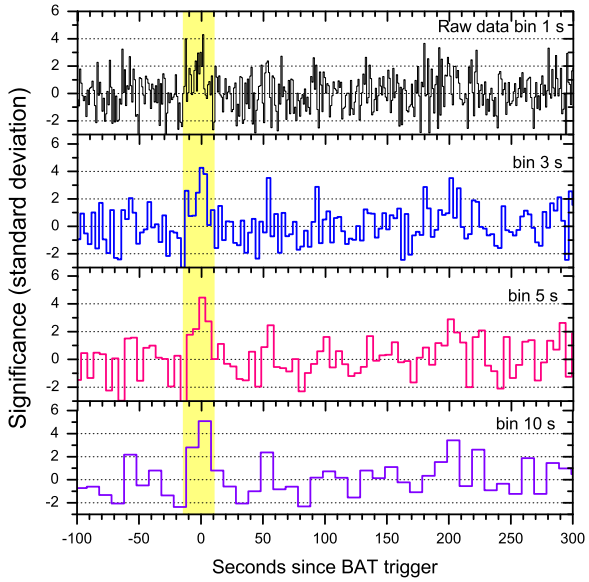

Figure 9. Statistical significance (number of standard deviations) of the 1 s, 3 s, 5 s, 10 s binning counting rate observed by the vertical Tupi telescope, as a function of the time elapsed since the *Swift* GRB140512A trigger time. The yellow band is only a visual guide.

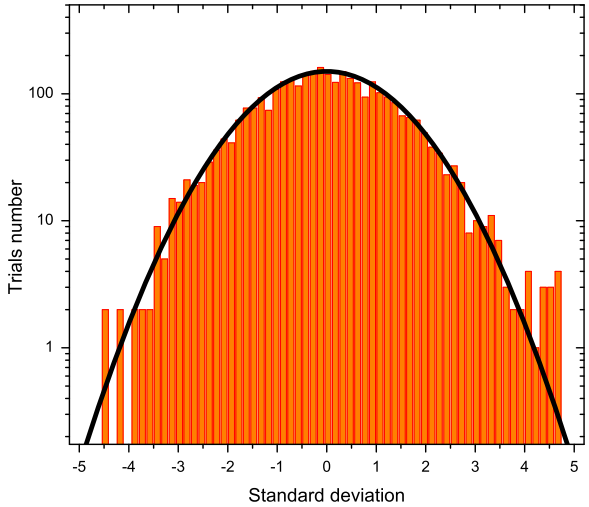

Figure 10. Distribution of the fluctuation counting rate for the vertical Tupi telescope (in units of standard deviations) using 1 s time windows inside a 1 hr interval (30 minutes before and 30 minutes after the trigger) around the *Swift* GRB140512A trigger time. The signals with a significance above 4σ are the Tupi signals associated with the *Swift* event. The background fluctuations are represented by the Gaussian distribution (solid line).

At high energies, the spectrum is well described as a power-law function with a steeper slope:

$$N(E) = A_{\gamma}E^{\beta}, \quad (3)$$

Table 2
Significance, Poisson Probability, and Annual Rate of a Muon Excess Being a Background Fluctuation

Event	Tupi-MAXI (Trigger 580727270)	Tupi-*Swift* (GRB140512A)
Significance (bin 5 s)	6.5 ± 0.9	4.5 ± 0.7
Probability (bin 5 s)	$(1.6 \pm 0.2) \times 10^{-9}$	$(7.40 \pm 1.21) \times 10^{-6}$
Annual rate	2.9	73.1

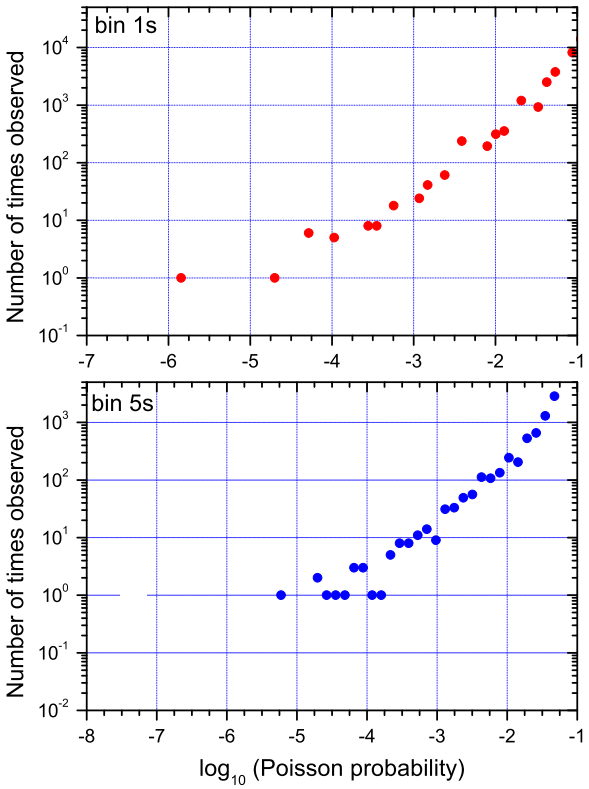

Figure 11. The Poisson probability distribution of the background fluctuations observed in the vertical Tupi telescope in a typical calm day (we assume that there are no astrophysical signals), using 1 s bins (top panel) and 5 s bins (bottom panel), respectively.

where $\alpha > \beta$, and the spectral parameters α, β, and E_0 vary from burst to burst. For instance, a "blast wave model," usually considered for GRB sources, is quite sensitive to the relationship between these two power-law indices.

We assume here that the energy spectrum of gamma rays above 10 GeV, that is, in the high-energy tail of a GRB, can be fitted by a single power-law function. There are two unknown quantities in the single-parameter power-law function, the coefficient A_γ and the spectral index β.

A convolution between the yield function S(E) (the number of muons per gamma ray is shown in Figure 12; Fasso & Poirier 2000) and the particle spectrum N(E) gives the response function, that is, the number of muons in the excess signal generated by the GRB photons during the time period T. This convolution can be expressed as

$$N_\mu = S_{\rm eff} \times T \int_{E_{\rm min}}^{\infty} S\left(E_\gamma\right) A_\gamma E_\gamma^{\beta} dE_\gamma. \quad (4)$$

Table 3
Number of Muons per Gamma Ray

R(km)	Tupi	YBJ
$R < 0.5$	$(97.8 \pm 2.9) \times 10^{-5}$	$(86.3 \pm 2.7) \times 10^{-5}$
$R < 1.0$	$(190.8 \pm 4.0) \times 10^{-5}$	$(185.9 \pm 4.0) \times 10^{-5}$
$R < 2.0$	$(276.2 \pm 4.8) \times 10^{-5}$	$(273.2 \pm 4.8) \times 10^{-5}$

Table 4
Number of Muons within a Given Radius, Divided by the Total Number of Muons

R(km)	Tupi	YBJ
$R < 0.5$	0.307 ± 0.010	0.267 ± 0.009
$R < 1.0$	0.600 ± 0.016	0.575 ± 0.015
$R < 2.0$	0.869 ± 0.021	0.845 ± 0.020

The specific yield function as a function of photon energy (assuming the vertical incidence) is determined according to the FLUKA[8] Monte Carlo results (Fasso & Poirier 2000). This FLUKA output can be described by the following fit:

$$S\left(E_\gamma > 10\ {\rm GeV}\right) = A_\mu E_\gamma^{\nu} \exp\left(-\left(E_0/E_\gamma\right)^{\lambda}\right), \quad (5)$$

where $A_\mu = (6.16 \pm 0.60) \times 10^{-5}$, $\nu = 1.183 \pm 0.014$, $E_0 = 7.13 \pm 0.56$ GeV, and $\lambda = 1.58 \pm 0.12$, as shown in Figure 6. Furthermore, the integrated time fluence can be obtained as

$$F = T\left[\int_{E_{\rm min}}^{\infty} dE_\gamma A_\gamma E_\gamma^{\beta} E_\gamma\right]. \quad (6)$$

5.1. Association with the MAXI Event

The terms on the left side of Equations (4) and (6) are known (see Table 1). Thus, we can consider all possible values of β and A_γ compatible with the observed muon excess value N_μ and the integrated fluence F. Figure 13 shows that one can obtain the best estimate for the spectral index using the intersection of two lines defined by Equations (4) and (6).

From this analysis we can find out that the best estimate for the spectral index is compatible with $\beta = -2.13 \pm 0.43$ and $A_\gamma = (3.34 \pm 0.67) \times 10^{-4} ({\rm cm^2\ s\ GeV})^{-1}$. In this case, the integrated time fluence (defined by Equation (6)) is $F = (2.10 \pm 0.42) \times 10^{-7}$ erg cm^{-2} in the gigaelectronvolt energy region. Considering that the second peak at $T_0 + 297.2$ s is a part of the same GRB, we can obtain the gamma-ray flux as 7.07×10^{-10} erg cm^{-2} s^{-1} or 29 mCrab.

[8] FLUKA ("FLUktuierende KAskade") is a detailed general-purpose tool for calculations of particle transport and interactions with matter.

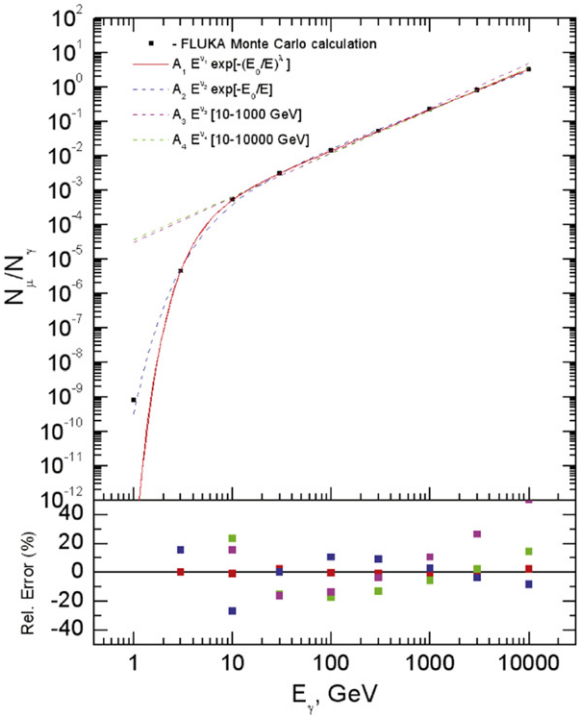

Figure 12. Yield function, as the number of muons at sea level per photon (vertical incidence), as a function of incident photon energy, from FLUKA calculations (black squares; Fasso & Poirier 2000). The lines show several fit functions. The bottom panel shows relative errors (in percent).

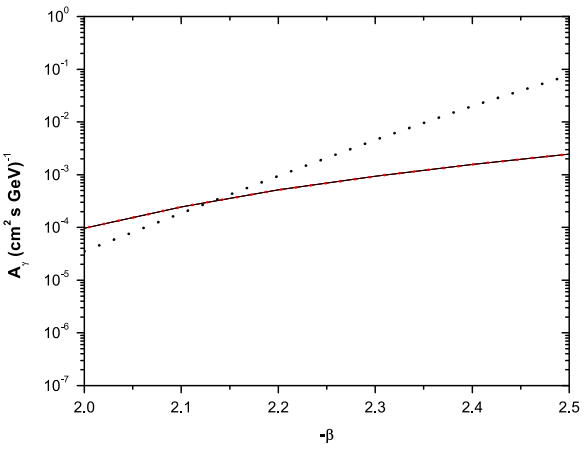

Figure 13. Correlation between the coefficient A_γ and the spectral index β for the MAXI–Tupi association. All possible values of A_γ and β compatible with the observed muon flux (dotted line) and the integrated fluence F (solid line) are obtained on the basis of Monte Carlo simulations and analytical calculations. These quantities are defined by Equations (4) and (6).

This value is in agreement with the gamma-ray flux reported by the MAXI team[9] (22 mCrab).

5.2. Association with the Swift Event

A similar analysis was made for the *Swift* GRB140512A event. In this case, the Tupi data is almost in coincidence with the *Swift* trigger time, and the significance in the raw data is 4.55σ, as shown in Figure 9 (top panel). The muon flux excess is estimated as $(8.7 \pm 1.6) \times 10^{-4}$ cm^{-12} s^{-1} sr^{-1} with a duration of 15 s, corresponding to the fluence above $(2.1 \pm 0.4) \times 10^{-6}$ erg cm^{-2}. The best estimate for the spectral index is compatible with $\beta = -1.86 \pm 0.15$ and $A_\gamma = (3.88 \pm 0.33) \times 10^{-5}$(cm^{-2} s GeV)$^{-1}$, as shown in Figure 14.

The integrated time fluence (defined by Equation (6)) is estimated as $F = (2.27 \pm 0.41) \times 10^{-5}$ erg cm^{-2} in the energy region above 10 GeV. This value is around twice as high as the fluence in the 15–150 keV band, obtained by the *Swift* team, as $(1.4 \pm 0.03) \times 10^{-5}$ erg cm^{-2} at the 90% confidence level. The *Swift* time-averaged spectrum from T-22.84 to T+186.29 s is best fit by a simple power-law model. The time-averaged gamma-ray spectrum in the 10−100 GeV energy band expressed in units of photons cm^{-2} s^{-1} can be obtained from the muon excess from T-12.5 s to T+2.5 s (integrating Equation (3)):

$$N_\gamma\left(>E_\gamma\right) = \int_{E_{\min}}^{E_{\sup}} dE_\gamma A_\gamma E_\gamma^{\beta}. \quad (7)$$

The result is shown in Figure 15. It is compared with the 1 s peak photon flux measured by *Swift* from T+121.96 s in the 15–150 keV energy band, measured as 6.8 ± 0.3 ph cm^{-2} s^{-1}. In this case, the power-law index of the time-averaged spectrum is 1.45 ± 0.04 (Sakamoto et al. GCN 16258). All of the quoted errors are at the 90% confidence level.

One can notice in Figure 15 the absence of data in the megaelectronvolt to gigaelectronvolt band. This does not mean that there are no photons in this energy range. Through the yield function it is possible to see that the effective energy threshold to the muon photoproduction is 10 GeV. Photons with the lower energies produce electron–positron pairs and can initiate electromagnetic showers (without muons) in the atmosphere. The particles that constitute the electromagnetic air shower (the soft component) are absorbed in the atmosphere, so they do not reach the ground level. Perhaps, balloon experiments with an adequate duty cycle could be suitable to detect photons from GRBs in the megaelectronvolt to gigaelectronvolt band.

6. THE TUPI EVENTS IN LIGHT OF THE FERMI LAT (>100 MeV) OBSERVATIONS

We examine the possibility of the ground observation of similar transient events within the FOV of the extended Tupi array of five telescopes. This study is extended to the events available in the GCN GRB database. We also perform a systematic comparison between the GRB characteristics observed by Fermi LAT (>100 MeV) and Fermi GBM (>50 keV; Ackermann et al. 2013). In particular, we look into the frequency of nonoccurrence of LAT-detected GRBs in the Tupi FOV.

6.1. The GRB Event Rate

The first Fermi LAT GRB catalog covers a 3 yr period starting from 2008 August (Ackermann et al. 2013). In this period, the Fermi GBM detects ~250 GRBs per year, and about half of them are within the Fermi LAT FOV. However, only ~10% were detected by the Fermi LAT (>100 MeV).

From 2013 September to 2014 May, the Tupi experiment has been continuously operating an extended array of five telescopes. In the period from 2013 September 8 to 2014 August 10, the Fermi LAT detected 19 GRBs (>100 MeV).

[9] So far there have been no reports on the light curve or the duration of the event.

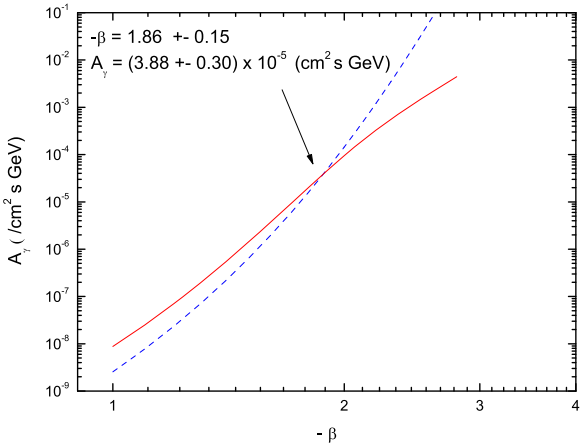

Figure 14. Correlation between the coefficient A_γ and the spectral index β for the *Swift*–Tupi association. All possible values of A_γ and β compatible with the observed muon flux (dotted line) and the integrated muon fluence F (solid line) are obtained on the basis of Monte Carlo simulations and analytical calculations. These quantities are defined by Equations (4) and (6).

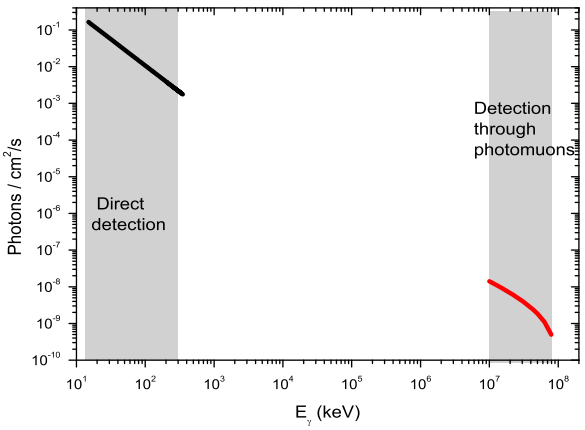

Figure 15. Peak photon flux (a power-law spectrum) for the *Swift* event GRB140512A (black bold line) in the 15–150 keV band (shaded area) and possible gigaelectronvolt counterpart spectrum obtained on the basis of the Tupi muon excess and the FLUKA Monte Carlo for a photoproduction process of the primary photon in the atmosphere (red bold line) in the 10–100 GeV band (shaded area).

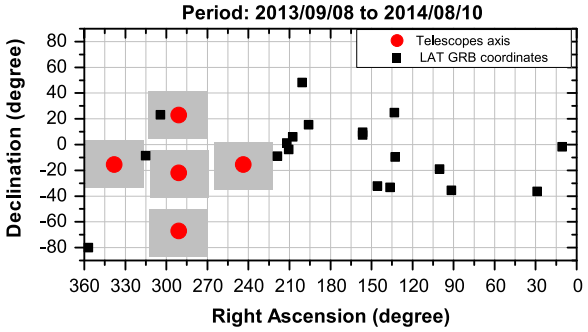

Figure 16. Equatorial coordinates show the positions of the five Tupi telescope axes at the GRB trigger time, as well as the Fermi LAT GRBs (>100 MeV) in the period from 2013 September 8 to 2014 August 10. The squares with circles represent the FOV of the Tupi telescopes. GRB131018B was within the FOV of the North Tupi telescope.

We found no report by Fermi on GRB emission from the MAXI event (trigger 580727270).

Figure 16 summarizes the situation, where the equatorial coordinates of the five Tupi telescope axes are shown with the GRB coordinates. The squares with circles represent the FOV of the Tupi telescopes.

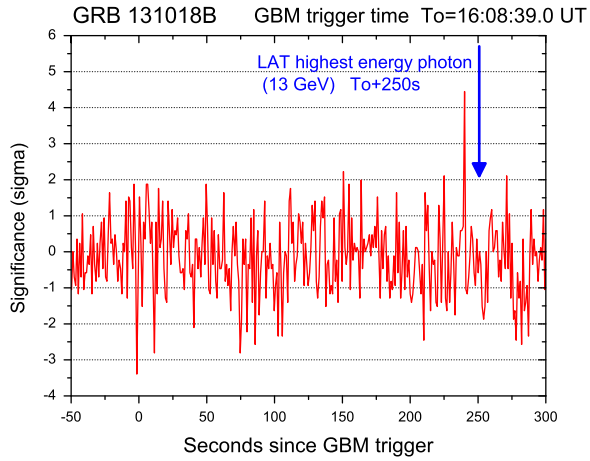

Figure 17. Statistical significance (number of standard deviations) of the 1 s binning counting rate observed by the North Tupi telescope, as a function of the time elapsed since the Fermi GBM GRB131018B trigger time (T_0).

The only LAT GRB coordinate within the FOV of the North Tupi telescope was at 16:08:39 on 18 October 2013, when the Fermi LAT detected high-energy emission from GRB131018B (Vianello et al. GCN 15357), which was also detected by the Fermi GBM (trigger bn131018673; Bin-Bin Zhang GCN 15360). The best LAT on-ground location is found to be (R.A., decl.) = 304.41, 23.11 (J2000), with a radius error of 0.13 deg. LAT did not actually trigger on GRB131018B; it was recovered in a ground analysis using the GBM information. More than 10 photons above 100 MeV were observed by LAT within 2000 s after the GBM trigger. The highest energy photon was a 13 GeV event that was observed 250 s after the GBM trigger. The trigger coordinates were within the FOV of the North Tupi telescope. We found a muon excess (a narrow peak) in association with this GRB, with a significance of 4.4σ, 240 s after the GBM trigger occurrence, as shown in Figure 17, where the 1 s binning muon counting rate is presented. We can see that the highest photon emission (observed by LAT) was about 10 s after the muon excess peak.

However, the signal looks like a spike, with a width of 1 s and a significance of 4.4σ. Under this condition, the Poisson probability of this signal being a background fluctuation is $p = 6.1 \times 10^{-5}$ or $\log 10P = 4.21$ (see Section 4). So, the daily rate of this type of event is 2.5 (912 per year).

We checked whether there were other possible muon excesses within the FOV of the telescopes corresponding to the GRB trigger time reported by *Swift* and Fermi GBM using the GCN database in the period from 2013 September 6 to 2014 May 13. In this period, there were 34 GRBs observed by satellites in the kiloelectronvolt energy region. The distribution of the number of GRB events observed by *Swift* and Fermi GBM within the FOV of the Tupi telescopes is shown in Figure 18. The majority of the events were compatible with the Tupi background fluctuations.

6.2. Delayed Onset of High-energy Emission

As indicated above, the detection by Tupi of the gigaelectronvolt counterpart of a GRB observed by spacecraft detectors would require a signal with a significance of at least 4σ and an

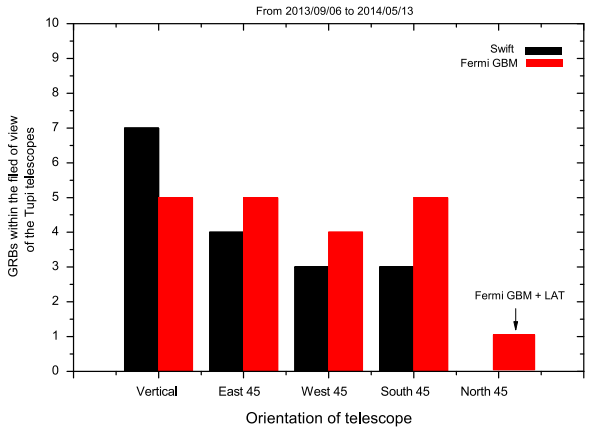

Figure 18. Distribution of the number of GRB events observed by *Swift* and Fermi GBM within the FOV of the Tupi telescopes in the period from 2013 September 6 to 2014 May 13.

onset time within the GRB T90 interval. Because of the high directionality of a typical GRB, it is also required that the signal is seen only by one of the telescopes. Coincident signals in two or more telescopes, in most cases, are related to solar transient events.

A delayed onset of the >100 MeV LAT emission with respect to the GBM-detected emission has been reported (Ackermann et al. 2013). A correlation between the T05 (>100 MeV) in the LAT and the T05 (>30 keV) in the GBM data shows a delay of up to ~50 s. However, photons above 100 MeV were observed within the 2000 s time interval after the trigger.

Similar systematics were observed in the three Tupi candidate counterparts of GRBs. The first candidate event (the MAXI event (trigger 580727270)) shows that the onset seen by Tupi was delayed by ~25.7 s with respect to the MAXI trigger time. In the second case (GRB131018B), the Tupi onset was delayed by 140 s with respect to the LAT trigger, and the highest photon was detected by LAT ~10 s after observation of the Tupi muon excess peak (see Figure 17). Finally, in the third case (GRB140512A), the Tupi signal is almost in coincidence with the *Swift* BAT trigger (see Figure 8).

6.3. Temporal Extension of the High-energy Emission

A correlation between the T90 (>100 MeV) values in the LAT and the T90 (50–300) keV values in the GBM shows that the duration of an event observed by the Fermi LAT is longer than the duration observed by the Fermi GBM. There were no reports on the duration of the MAXI event (trigger 580727270), so the systematics could not be verified. The T90 interval estimated by Tupi is ~6.1 s. However, if we take into account the second pick observed by the Tupi telescope, the T90 can be extended up to ~298 s.

In the case of GRB131018B, the GBM light curve shape is like that of a fast rising, exponential decay pulse with a duration T90 of ~38 s (50–300 keV). While the temporal extension of the burst emission in the LAT (>100 MeV) was above 2000 s, the highest photon (13 GeV) was detected after 250 s of the GBM trigger. This time is close to the muon peak observed by Tupi (~240 s after the trigger).

Finally, in the case of GRB140512A, there is practically no delay between the *Swift* BAT trigger time and the time of the Tupi peak.

On the other hand, the Fermi LAT indicates the power-law temporal decay at late times, dominated by a power-law spectral component. However, with no obvious pattern in the spectral evolution, the photon spectral index typically averages around the value of −2. This is in agreement with the photon spectral index of -2.13 ± 0.43 obtained on the basis of the Tupi data for the MAXI event (trigger 580727270).

6.4. Highest-energy Detected Photons

The LAT-detected GRB emission frequently reaches energies of several tens of gigaelectronvolts. Photons with energies above 10 GeV have been observed in at least eight GRBs.

The presence of gigaelectronvolt photons in the LAT events is favorable for the GRB detection at ground level. If there are GRB photons with energies above 10 GeV, then it is possible to detect the muon excess at the ground (as in the Tupi experiment) due to photonuclear reactions in the Earth's atmosphere,

6.5. Fluence at High and Low Energies

It was shown that in long GRBs the LAT fluence is about 10% of the GBM fluence. On the other hand, in short GRBs the LAT fluence is higher than the GBM fluence.

Because there is no report on the MAXI event light curve and its duration, we can use indirect methods. First, let us consider only the first peak observed by Tupi. Taking into account that $T90 = 6.1$ s, where T90 is the Tupi estimate, a fluence can be calculated as $F = (2.1 \pm 0.42) \times 10^{-7}$ erg cm^{-2}. If we consider the second Tupi peak as well, then the Tupi fluence would be ~29 m CraB, which is very close to the MAXI team value.

Our preliminary fluence estimate for the Tupi candidate in association with GRB140512A is $\sim 2.4 \times 10^{-5}$ erg cm^{-2}. This value is close to $1.4 \pm 0.03 \times$ erg cm^{-2}, which is the fluence reported by *Swift* BAT using the 15–150 keV band (Sakamoto et al. GCN 16258).

6.6. Deficit of High-energy Emission from GRBs

As previously mentioned, about half of the GBM GRBs occur in the LAT FOV. However, only ~10% are detected with the LAT (above 100 MeV). The situation becomes critical in the case of Tupi. Only a small fraction of GRBs in the kiloelectronvolt energy region (~4%) are in the Tupi FOV with a signal significance above 4σ. In order to produce muons detected at ground level (the Tupi experiment), photons with energies above 10 GeV are required. Several reasons have been suggested to explain the deficit of events, for instance, the possibility of existence of a spectral cutoff in some GRBs, or the softening of the spectral index β. In addition, the high energy suppression in the tail of the energy spectra can be linked either to the internal opacity effects in GRB emission or to the intergalactic medium, imposing limits on the bulk Lorentz factor. One can also consider the possibility that there may be some other physical processes, as well as the diversity in the intrinsic GRB properties, leading to a situation that the transients observed by Tupi are not the same type of gigaelectronvolt emission seen by LAT.

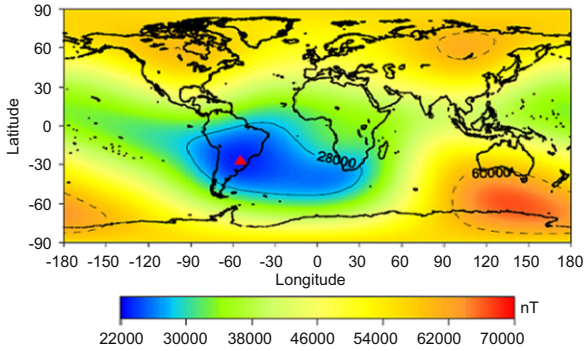

Figure 19. Geographic distribution of geomagnetic field intensity. The SAA boundary is around $B = 28{,}000\,nT$. The red triangle indicates the location of the SAA central region ($26°S$, $53°W$) and is the area where the magnetic field is less than $B = 28{,}000\,nT$.

6.7. Possible Contamination from Solar Events

The current time period corresponds to the solar cycle 24. On 2013 October 15, in the period from 01:40 UT to 23:31 UT, in total 15 solar flares were observed (http://www.lmsal.com). Twelve of these flares[10] were C class (minor, without influence on Earth) and three flares were M class (medium). There was no flare close to the MAXI event (trigger 580727270) onset at 21:55 UT. The nearest (in time) C-class solar flare ended at 20:57 UT, before the MAXI event, and the next solar flare (M class) started at 23:31 UT. A similar situation has been observed for the *Swift* event GRB140512A (trigger = 598819) at 19:31:49 UT. On 2014 May 12, six C-class solar flares were observed, four of them in the period from 01:33 to 07:44 UT, one started at 17:56 UT and ended at 18:11 UT, and the last one started at 22:09 UT. In addition to that, no other transient events were found, nor any anomalous changes in the atmospheric pressure, temperature, or other environmental conditions known to us during the time period close to the detection of the GRB candidate events.

7. IS THE SAA FAVORABLE TO DETECT GAMMA-RAY BURSTS?

In the SAA central region, $26°S$, $53°W$, the shielding effect of the magnetosphere has a "dip," with an anomalously weak geomagnetic field strength of 22,000 nT (Barton 1997), as shown in Figure 19, where the geographic distribution of the geomagnetic field intensity is presented. We can see that the geomagnetic field is significantly lower in the SAA compared to elsewhere in the world (Macmillan et al. 2009; Casadio & Arino 2011).

In the SAA, the Earth's inner Van Allen radiation belt comes closest to the Earth's surface (Barth 1997; Casadio & Arino 2011). The Van Allen radiation belts are symmetric with respect to the Earth's magnetic axis. The Earth's magnetic axis is tilted with respect to the Earth's rotational axis by an angle of 11°. The magnetic axis is offset from the rotational axis by ~400 km. As a result of the nonconcentricity and tilt of the Earth rotation axis and its magnetic dipole, the inner Van Allen belt is closest to the Earth's surface over the South Atlantic Ocean. The shape of the SAA evolves with time, and its size varies with altitude.

[10] Flares are classified into X, M, C, B, and A flares, with X corresponding to the GOES satellite flux in excess of 10^4 W m^{-2} at Earth, with successive classifications decreasing in decades.

A consequence of the severe reduction of the magnetic field in the SAA is that primary high-energy charged particles penetrate deeper into the upper atmosphere there than anywhere else on Earth. It has also been shown that the SAA region is prone to increased ionospheric ionization by the precipitation of high-energy particles from the inner Van Allen belt (Cilliers et al. 2006). The enhanced particle precipitation in the SAA region causes an increase in the ionospheric conductivity, growth of the conductivity gradients, and, as a result, generation of strong local electric fields (Dmitriev & Yeh 2008).

There is at least one more factor favorable to conducting gamma-ray astronomy within the SAA region. The effect is related to the lateral spread of particles at the level of observation.

7.1. Magnetic Lateral Effect

Nuclear active particles, such as pions, are produced in nuclear interactions. Thus, a pion after its production is characterized by a momentum $p = (p_{\parallel}^2 + p_{\perp}^2)^{1/2}$, where $p_{\perp}$ is the transverse momentum and $p_{\parallel}$ is the longitudinal momentum. Particles with momentum p, produced at the altitude z, have a lateral spread at the observation level as

$$r = \left(\frac{p_{\perp}}{p_{\parallel}}\right) z. \tag{8}$$

Because pion decay is the main mechanism for the production of muons, the pion's transverse momentum is transferred to the muon. Thus, the transverse momentum is the main cause of the angular divergence of muons, and the lateral spread by this effect is as large as several tens of meters. In addition, charged particles such as electrons and muons traversing a finite thickness of matter suffer repeated elastic Coulomb scattering. The cumulative effect of these small-angle scatterings is a net deflection from the original particle direction. The mean-squared angle of multiple scattering of a muon with energy E_{μ} can be approximated (Olbert 1954) as

$$\langle\theta^2\rangle^{1/2} \approx \sqrt{5.8\ \mathrm{MeV}/E_{\mu}}, \tag{9}$$

which is about 4.4° for $E_{\mu} = 1.0$ GeV.

However, there is an additional source for the lateral dispersion of particles. This is the Earth's magnetic field (De los Reyes et al. 2006). Let us consider a bundle of photons ($E_{\gamma} > 10$ GeV) incident vertically at the top of the atmosphere. The muons, produced in the atmosphere by photoproduction, tend to travel in the downward direction. As the muon travels, it will be shifted by a horizontal distance Δr in the direction perpendicular to the Earth's magnetic field B:

$$\Delta r \sim z^2/R = z^2 ceB/p, \tag{10}$$

where z is the height of the atmosphere where the muon is generated, and R is the radius of curvature of an (initially) vertical positive muon traveling downward in the atmosphere with momentum p. The magnetic field strength in the SAA central region is at least two times smaller than that outside the SAA. As a result, the number of collected muons in a telescope located near the SAA central region is higher.

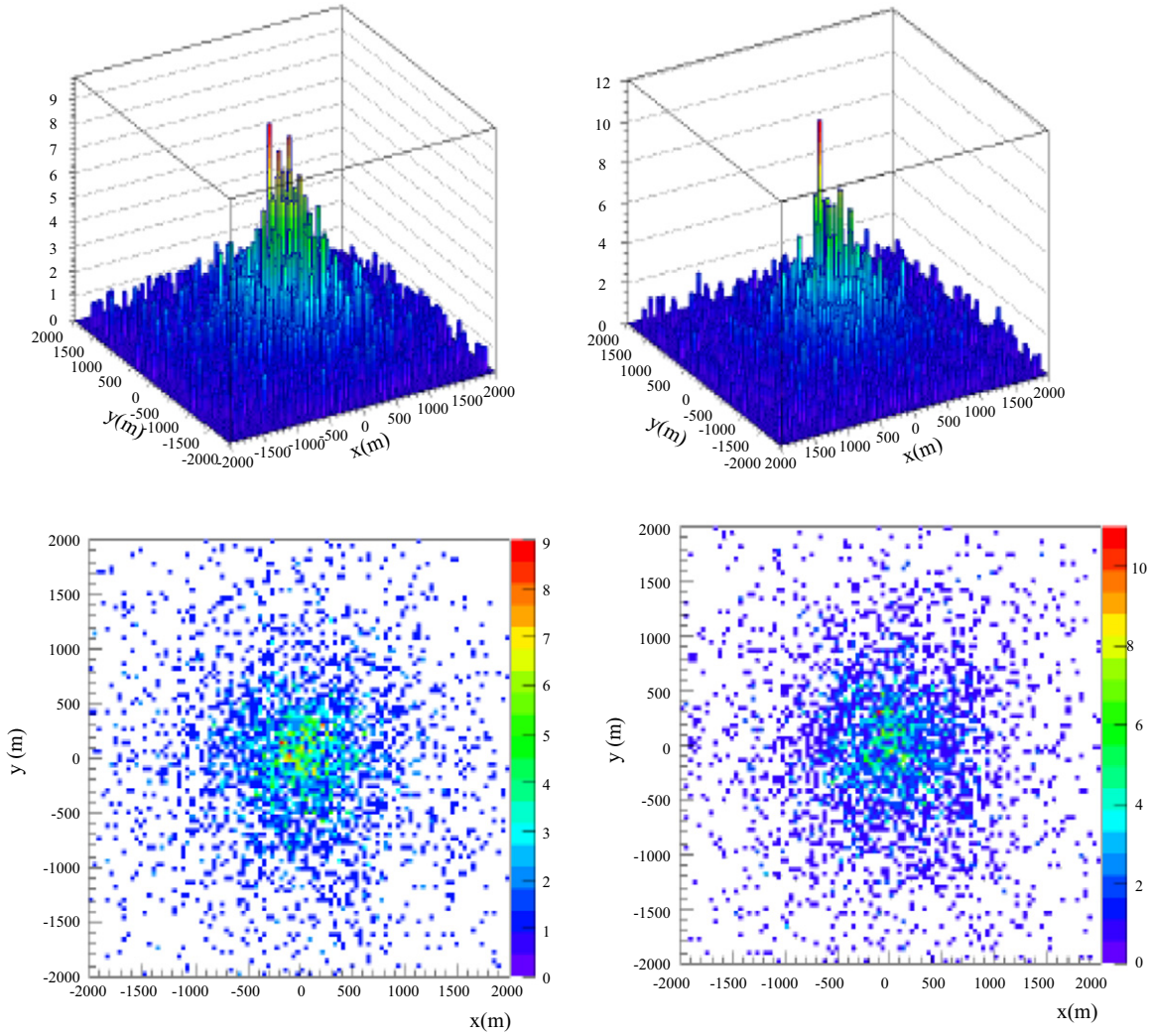

Figure 20. Lateral dispersion of muons (E > 0.1 GeV) at sea level in air showers initiated by 30 GeV photons. The top panel shows the three-dimensional (3D) and the bottom panel shows the two-dimensional (2D) scatter plot. Left plot: the geomagnetic conditions of the Tupi experiment within the SAA region. Right plot: the geomagnetic conditions of the Yangbajing cosmic-ray station at Tibet, China, 4300 m above sea level. The color-coded histogram shows the number of events. The bottom panel shows a 2D scatter plot, where the x coordinate and the y coordinate display distance in meters on the horizontal plane. The top panel shows a 3D plot, where the z axis displays the number of events.

The lateral dispersion of muons, their scattering at sea level, and the effect that is due to Earth's magnetic field are studied in the present survey.

7.2. Simulation Parameters

Using FLUKA (Fasso & Poirier 2000) and CORSIKA[11], we performed a Monte Carlo simulation to produce muons at sea level with the energy threshold of 100 MeV.

In order to study the effect of Earth's magnetic field on the lateral dispersion of muons at sea level, we estimate the number of muons expected at sea level at two sites with different geomagnetic conditions. The first site has the geomagnetic conditions of the Tupi experiment (located in Niteroi, Brazil), and the second one, called YBJ hereafter, has the geomagnetic conditions of Yangbajing International Cosmic Ray Observatory at Tibet, China, 4300 m above sea level. The geomagnetic field components (horizontal, vertical) at these two sites are, respectively,

1. Tupi: $B = (18.13, -14.60)$ mT;
2. YBJ: $B = (34.13, 36.54)$ mT.

We have simulated 1.2×10^6 showers for each site. The primary photon energy was set to 30 GeV, and the muon energy threshold was 100 MeV. Only the vertical incidence of photons is considered in the present simulation.

7.3. Results

Tables 3 and 4 below show the number of muons N_μ produced within a given radius per gamma ray, the ratio N_μ/N_T, where N_μ is the number of muons produced within a given radius range, and N_T is the total number of muons produced by the photons, for each site.

The output of the muon lateral distribution is shown in Figure 20.

[11] COsmic Ray Simulations for KAscade (CORSIKA) is physics computer software for simulation of extensive air showers initiated by high-energy cosmic particles (http://www.ikp.kit.edu/corsika/).

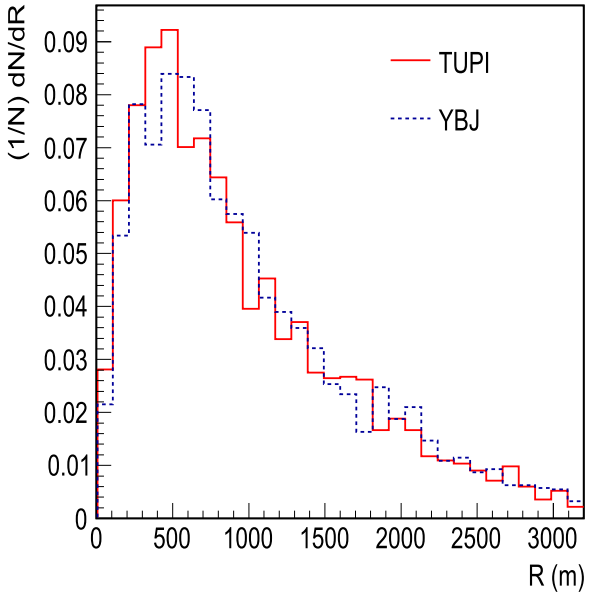

Figure 21. Normalized lateral distribution of muons at the surface measured from the shower axis. Solid line: Tupi; dashed line: YBJ.

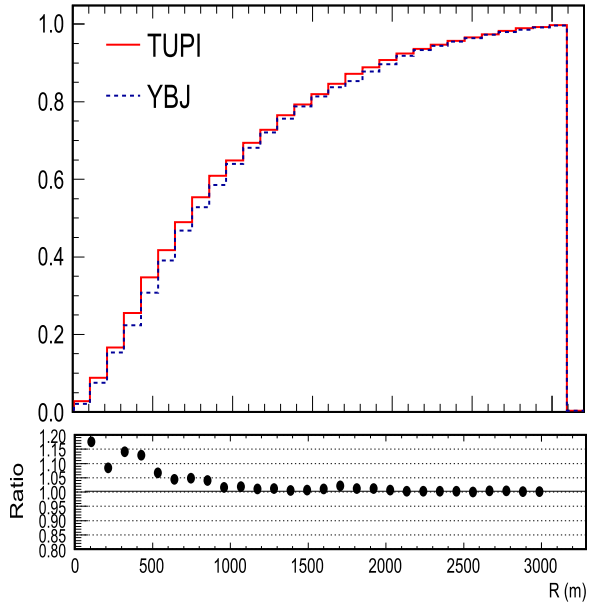

Figure 22. Cumulative distribution of the normalized lateral distribution of muons (top panel) and their ratio (bottom panel). Solid line: Tupi; dashed line: YBJ.

The lateral distribution of muons at the surface measured from the shower axis is presented in Figure 21. Most of the events are situated within ∼0.5 km. The YBJ distribution is approximately flat at $R < 1.0$ km.

Figure 22 shows the cumulative distribution of the normalized lateral distribution of muons in the Tupi and YBJ events (top panel) and their ratio (bottom panel). As can be seen from Figure 22, the number of muons at $R < 0.5$ km can be ∼15% higher in the case of Tupi.

8. CONCLUSIONS

We have reported the description and analysis of a muon excess flux in temporal and spatial correlation with triggers from space-based missions that were reported through the GCN. The first is associated with the unknown X-ray transient event (trigger 580727270) observed on 2013 October 15 by the MAXI instrument on the ISS, and the second is associated with the GRB GRB140512A observed on 2014 May 12 by the *Swift* satellite. In both cases, the muon excess has a signal significance above 4σ, even when the time profiles of their counting rates were binned with a temporal width above 5 s. This means that the signals are not spikes with a width around 1 s, such as used in the data acquisition. In addition, a triggered analysis at ground level, independent of satellite observations, was described. We would like to point out that both events analyzed in this survey meet the established criteria (untriggered and triggered) to be considered as the gigaelectronvolt counterparts of GRBs.

The Tupi muon telescopes are sensitive to primary particles (including photons) with energies above the pion production threshold. They can register muons at sea level with energies greater than ∼0.1 GeV. The Tupi experiment is located at sea level and within the SAA region, where the shielding effect of the magnetosphere has a "dip" that is due to the anomalously weak geomagnetic field strength. A Monte Carlo calculation shows that the atmospheric lateral spread of photomuons at ground level is narrow and the number of muons is high in the SAA region. These favorable experimental conditions can increase the telescope's sensitivity and allow the detection of signals from GRBs at ground level.

Based on Monte Carlo simulations and analytical calculations, we estimated the primary gamma-ray spectrum and the integrated time fluence of the burst (the MAXI transient event) as $F = (2.10 \pm 0.42) \times 10^{-7}$ erg cm^{-2}. This fluence is for the high-energy emission (photons with energies above 10 GeV). However, considering that the second peak at $T_0 + 297.2$ s is a part of the same GRB, we can estimate the expected gamma-ray flux as 7.07×10^{-10} erg cm^{-2} s^{-1} or 29 mCrab. This value is in agreement with the gamma-ray flux of 22 mCrab reported by the MAXI team. In the case of the *Swift*–Tupi association, the estimated fluence was $F = (2.27 \pm 0.41) \times 10^{-5}$ erg cm^{-2}. This value is higher than the fluence $(1.4 \pm 0.03) \times 10^{-5}$ erg cm^{-2} at the 90% confidence level obtained by the *Swift* team in the 15–150 keV band.

On the other hand, from a systematic characteristics study between the GCN (kiloelectronvolt) GRBs including the MAXI events within the FOV of the extended Tupi array and their probable gigaelectronvolt counterparts seen by Tupi, we show that these characteristics are not far from the systematics observed in the Fermi LAT (>100 MeV) GRBs and their kiloelectronvolt Fermi GBM counterparts, as reported in the first Fermi LAT GRB catalog. In some cases, the nondetection of the high-energy component may be due to several physical reasons that require further clarification and future studies. More statistics and further experiments are needed to replicate the Tupi findings.

We would like to thank the referee for the thorough evaluation of the manuscript, valuable comments, and practical suggestions that have significantly improved the original text. This work is supported by the National Council for Research (CNPq) of Brazil, under grants No. 306605/2009–0 and No. 01300.077189/2008–6 and Fundacao de Amparo a Pesquisa do Estado do Rio de Janeiro (FAPERJ) under grant No.

08458.009577/2011–81. This research has made use of data provided by the MAXI and *Swift* teams. We express our gratitude to the Goddard Space Flight Center for valuable information and data used in this study through the GCN web page (http://gcn.gsfc.nasa.gov/).

REFERENCES

Abdo, A. A., Ackermann, M., Arimoto, et al. 2009, Sci, 1688, 323
Abdo, A. A., Ackermann, M., Ajello, et al. 2009b, ApJL, 706, L138
Abdo, A. A., Allen, B. T., Berley, D., et al. 2007a, ApJ, 666, 361
Abdo, A. A., Allen, B. T., Berley, D., et al. 2007b, ApJL, 664, L91
Abdo, A. A., Allen, B. T., Berley, D., et al. 2007c, ApJL, 658, L33
Ackermann, M., Ajello, M., Asano, et al. 2013, ApJS, 209, 11
Augusto, C. R. A., Kopenkin, V., Navia, C. E., Tsui, K. H., & Sinzi, T. 2012a, PhRvD, 86, 022001
Augusto, C. R. A., Kopenkin, V., Navia, C. E., et al. 2012b, ApJ, 759, 143
Augusto, C. R. A., Kopenkin, V., Navia, C. E., et al. 2013, PhRvD, 87, 103003
Augusto, C. R. A., Navia, C. E., Shigueoka, H., & Tsui, K. H. 2011, PhRvD, 84, 042002
Augusto, C. R. A., Navia, C. E., Tsui, K. H., Shigueoka, H., & Miranda, P. 2010, APh, 34, 40
Barth, J. L., Dyer, C. S., & Stassinopoulos, E. G. 2003, IEEE Transactions on Nuclear Science, Vol. 50, 466
Barton, C. E. 1997, JGG, 49, 121
Casadio, S., & Arino, O. 2011, AdSpR, 48, 1056
Cilliers, P. J., Mitchell, C. N., & Opperman, B. D. L. 2006, in Meeting Proc. RTO-MP-IST-056 28, Meeting on Characterising the Ionosphere (Neuilly-sur-Seine, France: RTO)
Dmitriev, A., & Yeh, H. C. 2008, AnGp, 26, 867
De los Reyes, R., Ona-Wilhelmi, E., Contreras, J. L., Jager, O. C., & Fonseca, M. V. 2006, IJMPA, 20, 7006
Fasso, A., & Poirier, J. 2000, PhRvD, 63, 036002
Frontera, F., Amati, L., Costa, E., et al. 2000, ApJS, 127, 59
Gehrels, N. 2004, ApJ, 611, 1005
Girolamo, T. D., Vallania, P., Vigorito, C., et al. 2008, in Proc. 30th ICRC 3, ed. R. Caballero et al. (Mexico City, Mexico: UNAM), 1163
Gotz, D., Mereghetti, S., Beck, M., Borkowski, J., & Mowlavi, N. 2003, GCN Circ., 2459, 1
Hurley, K., Dingus, B. L., Mukherjee, et al. 1994, Natur, 372, 652
Kumar, P., & McMahon, E. 2008, MNRAS, 384, 33
Macmillan, S., Turbitt, C., & Thomson, A. 2009, AnGp, 52, 83
Matsuoka, M., Kawasaki, K., Ueno, S., et al. 2009, PASJ, 61, 999
Mitrofanov, I. G., Litvak, M. L., Briggs, M. S., Paciesas, W. S., & Pendleton, G. N. 1999, ApJ, 523, 610
Olbert, S. 1954, PhRv, 96, 1400
Panaitescu, A., & Meszaros, P. 2000, ApJL, 544, L17
Preece, R. D., Briggs, M. S., Mallozzi, R. S., Pendleton, G. N., & Paciesas, W. S. 1998, ApJL, 506, L23
Pe'er, A., & Waxman, E. 2004, ApJL, 603, L1
Racusin, J. L., Karpov, S. V., Sokolowski, et al. 2008, Natur, 455, 183
Soderberg, A. M., Kulkarni, S. R., Berger, S., et al. 2004, Natur, 430, 648
Wang, X. Y., Dai, Z. G., Lu, T., et al. 2001, ApJL, 546, L33
Zhang, B., & Meszaros, P. 2001, ApJ, 559, 110